Reconstruction on Si(100) surfaces

Young Joo Lee and Sehun Kim
Department of Chemistry and Center for Molecular Science, Korea Advanced Institute of Science and Technology, Taejon, Korea

Chi-Sun Hwang and C. Lee
Department of Physics, Korea Advanced Institute of Science and Technology, Taejon, Korea

Chanyong Hwang*
Materials Evaluation Center, Korea Research Institute of Standards and Science, P.O. Box 102, Yuseong, Taejon, Korea
(Received 14 April 1994)

We have observed several reconstructions on a Si(100) surface with different annealing procedures. The observed reconstructed phases are the coexistence of the (2×2) phase and the (2×8) phase after high-temperature ($\gtrsim 950$ K) annealing followed by quenching, and the half-order streak with the presence of the (2×1) phase after low-temperature ($\lesssim 950$ K) annealing. The phase transition from the metastable (2×2) and (2×8) phases to the stable half-order streak is reversible upon annealing temperature and cooling rate. The distribution of kinks and missing dimer defects is expected to be the main cause of these reconstructions.

It has been generally believed that the (2×1) phase found on a Si(100) surface originates from symmetric dimers or buckled dimers.[1,2] Hamers, Tromp, and Demuth showed by scanning tunneling microscopy (STM) with high lateral resolution that far from defects, symmetric dimers are observed, while buckled dimers are observed near steps and defects.[3] Buckling direction is not ordered in the long range but some local $p(2\times2)$ or $c(4\times2)$ structure has been reported. Especially the $c(4\times2)$ phase is known to appear either by very slow cooling after high-temperature annealing,[4,5] or by cooling down to below 200 K.[2,6,7] The $c(4\times2)$ phase observed at low temperature is transformed to a (2×1) phase with increasing temperature up to ambient, where a half-order streak appears during the transition.[6,7] This phenomenon has been explained by an order-disorder phase transition in the buckling direction. The half-order streak was reported also at room temperature by He atom diffraction.[8] Weiss, Schmeisser, and Göpel reported a clear $p(2\times2)$ low-energy electron diffraction (LEED) pattern after high-temperature annealing of a surface misoriented by 0.5° but the origin was not explained in their work.[9] Higher-order $(2\times n)$ phase reconstruction, where the n is an integer ranging from seven to nine, has been reported by quenching the surface from high temperature.[10,11] On a single stepped vicinal Si(100) surface, there are two types of steps and also two types of terraces depending on the dimer row direction with respect to the step edge. According to Chadi's notation, for S_A steps, dimer rows on the upper terrace are parallel to the step edge and for S_B they are perpendicular.[12] For the A terrace, dimer rows are parallel to the step edge and for the B terrace they are perpendicular. In this paper, we will show the appearance of different phases and their reversible phase transition upon heating and cooling. Also, the role of defects and steps in the reconstructions will be discussed.

The measurements of the reconstructed phases and their reversible phase transition were made with conventional four-grid LEED optics combined with a CCD (charge-coupled device) under a working pressure less than 2.5×10^{-10} Torr. The CCD enables us to measure the diffracted beam intensity and the shape quantitatively. The sample used in this experiment is a commercial mirror-polished Si(100) wafer ($15\times5\times0.38$ mm^3) misoriented by 0.5° toward the [011] direction. After Ar^+-ion sputtering and annealing followed by flashing up to 1450 K, we could see a two-domain (2×1) LEED pattern. To see the effect of annealing conditions on surface reconstruction, we have varied the annealing temperature between 600 and 1400 K, and the cooling rate between 0.5 K/sec and radiation quenching (~ 150 K/sec). Also, defect density was varied by bombarding Ar^+ ions onto the surface with different ion energies, ion doses, and annealing time after bombardment. The ion energies that we used are 0.6, 0.8, 1.0, 1.5, and 2.0 keV with the fixed dose of 1.0×10^{16} ions/cm^2. The ion doses are varied among 2.1×10^{15} ions/cm^2, 2.0×10^{16} ions/cm^2, 7.2×10^{16} ions/cm^2, and 1.0×10^{17} ions/cm^2 at the fixed ion energy of 2.0 keV. The surface atomic density of Si(100) is about 6.78×10^{14} atoms/cm^2.

The observed reconstructions are as follows. First, (2×2) and (2×8) LEED patterns always appeared simultaneously after high-temperature ($\gtrsim 950$ K) annealing followed by rapid cooling. Second, a half-order streak is observed after low-temperature annealing ($\lesssim 950$ K), irrespective of cooling rate. The streak pattern was also observed after high-temperature annealing followed by slow cooling. Figure 1 represents a phase diagram on the different annealing temperatures and cooling rates. The phases are reversible upon their own annealing temperature and cooling rate, and independent of annealing time

0163-1829/94/50(15)/11204(4)/$06.00

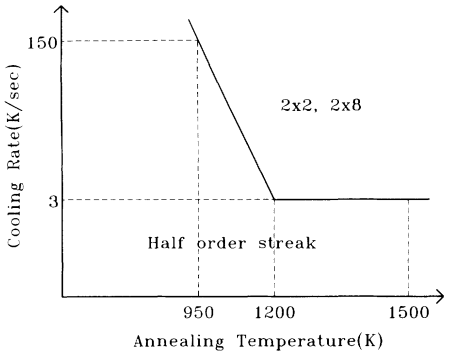

FIG. 1. The structural phase diagram constructed from LEED data with the different annealing temperatures and the different cooling rates. The value of 150 K/sec corresponds to the radiation quenching, and the 1500 K represents accessible maximum value.

between 1–10 min for the high-temperature annealing and between 8 min to 3 h for the low-temperature annealing.

The (2×2) pattern was observed only below 30 eV of electron beam energy, while the (2×8) pattern appeared up to high energy. The (2×2) beams are weak and somewhat diffuse [Fig. 2(a)], which means that the reconstruction occurs in local regions but the domain size is large enough to give a clear diffraction pattern. A clear (2×2) phase has not been reported except in the work of Weiss, Schmeisser, and Göpel in their diffraction experiment.[9] The buckled dimers sometimes form local $p(2\times2)$ or $c(4\times2)$ structures.[3] The observed (2×2) pattern can be assigned to a $p(2\times2)$ structure due to its energy lower than that of the $c(2\times2)$ structure,[13] and the absence of $c(2\times2)$ structure in the reported STM data. The $c(4\times2)$ structure was not observed in our study. In the (2×8) pattern [Fig. 2(b)] the eighth-order spots only near the half-integer- or integer-order spots are very intense. This is consistent with the previous reports that the (2×8) phase is ascribed to an *ordered-defect arrangement* where the missing dimers are lined up.[10,11] Two intensity profiles from two directions [Fig. 2(c)] show that the phase is equally populated on two types of terraces separated by an odd number of monoatomic steps. When this surface, where the $p(2\times2)$ and the (2×8) phase coexist, is annealed at low temperature, the surface undergoes a reversible phase transition to a half-order streak (Fig. 1). The structural phase transition will be discussed later.

For the half-order streak (Fig. 3), an intensity profile and photograph shows three features. First, the intensity ratio of the streak to the integer-order spot is about 0.2, and the integrated intensity of this streak is weaker than that of half-order spot. Second, the intensities of these two half-order streaks from the two types of terraces are nearly the same. Third, the line shape of the half-order streak is very broad compared with that of the integer order. From above three features, we know the coexistence of this streak phase with the (2×1) phase and the equal population of this phase on two types of terraces, and that the one-dimensional ordering must be restricted in length. The origin of this half-order streak is attributed to the one-dimensional ordering of the buckling direction in buckled-dimer domains that will be discussed later.

In order to explain the observed reconstructions fully, missing dimer defects and step fluctuation should be considered. For missing dimer defects, there is an equilibrium number of defects on two types of terraces due to the

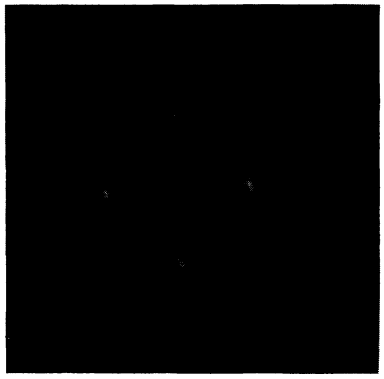

(a)

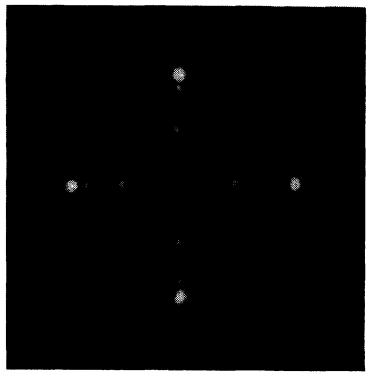

(b)

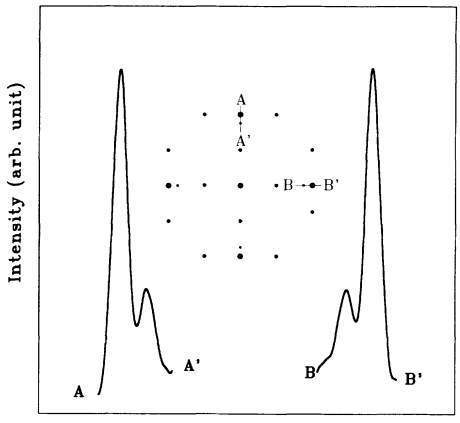

(c)

FIG. 2. The photographs and line profile of a LEED pattern for radiation quenched surface. (a) (2×2) at $E=23$ eV. (b) (2×8) at $E=39$ eV. (c) The line profile of a (2×8) LEED pattern represented in (b). The line scan direction is shown in the inset of (c), where the inset is schematic of photograph of (b).

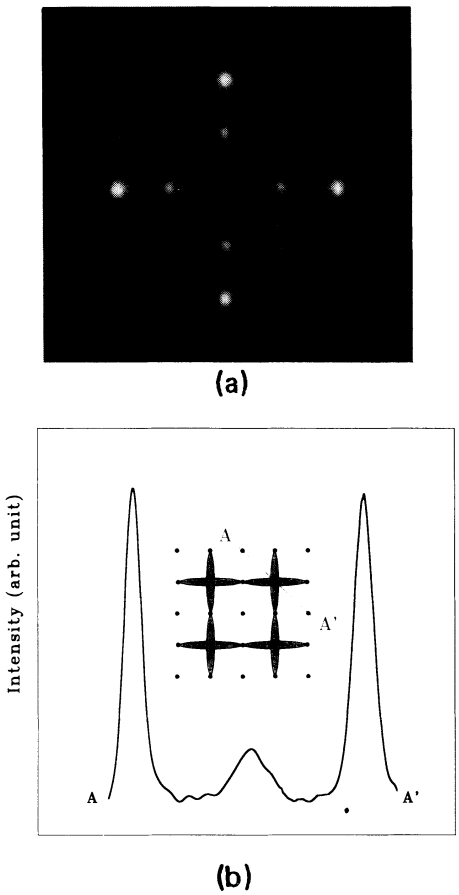

FIG. 3. The photograph and line profile for a slow-cooled surface. (a) The LEED pattern of half-order streaks at $E=39$ eV. (b) The line profile of this LEED pattern from the direction represented in the inset of (b).

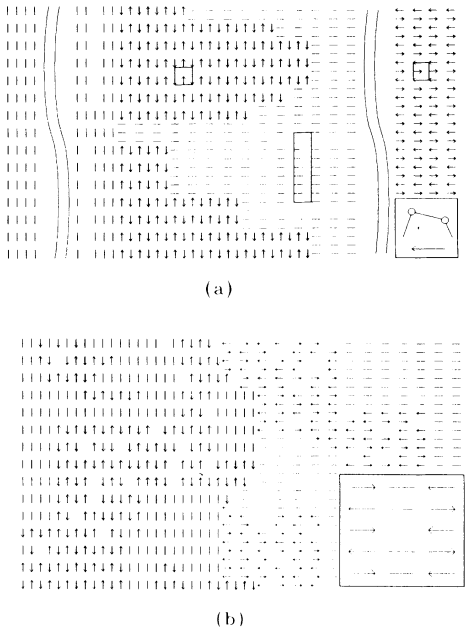

FIG. 4. The proposed model surface that can explain the observed reconstructed phases dependent on the annealing temperature and the cooling rate. See text for a detailed explanation. In (a) and (b), the left-hand side represents the upper terrace and the nominal S_B step is located at the middle and nominal S_A step at the ends of both sides. (a) A schematic diagram of the domains giving the $p(2\times2)$ and the (2×8) phases for radiation quenched surface from high temperature. The arrow represents the buckled dimer and the buckling direction is shown in the inset. (b) A schematic diagram of the domains giving the half-order streak and the (2×1) phase for the low-temperature annealed or slowly cooled surface, where the density of defects is not homogeneous. The buckling direction near one missing dimer is represented in the inset of (b).

tendency of lowering the surface free energy by reducing the number of dangling bonds with missing dimer creation.[14] These defects are believed to be ordered or disordered depending on annealing temperature. At high temperature ($\gtrsim 950$ K), the defects are ordered to relax strain energy. The dimers are continuously missed along the dimerization direction and the missing dimer lines occur every eighth period in the direction perpendicular to the dimerization, which relax the compressive strain energy [Fig. 4(a)].[10,11] The observed (2×8) phase is ascribed to this ordered-defect arrangement. At low temperature ($\lesssim 950$ K), the defects are disordered and the distribution of defects is not homogeneous as shown in Fig. 4(b). This is in good agreement with the STM picture by Hamers, Tromp, and Demuth.[3] The (2×1) phase originates from the symmetric-dimer domains where the density of defects is very low, while the phase of the half-order streak originates from the buckled-dimer domains containing some high density of defects which are randomly distributed. We construct the buckling directions in the buckled-dimer domains, based on the previous reports.[15,16] First, the two dimers in the next rows of the missing dimer are pulled in toward the vacancy [inset of Fig. 4(b)]. Second, the two buckled dimers initiate the buckling with a strong zigzag correlation along the dimer rows. Since the defect distribution is random, the buckled dimers cannot be correlated across the dimer rows. So the buckled-dimer domain produces a one-dimensional disorder across the dimer rows and gives "two" times the periodicity along the dimer rows in the buckling direction. The correlation along the dimer rows is restricted in length and this is the cause of the broadness of the streak mentioned previously.

For step fluctuation, STM studies on single stepped surfaces showed that the S_B step fluctuated more than the S_A step due to the different formation energy of the two types of steps,[17] and the S_A step edges induced strong buckling of dimers.[3] Furthermore, recent high-temperature STM studies shows that the nominal S_B step becomes more rough with increasing temperature ($\lesssim 700$ K).[18] This rough S_B step contains a lot of long S_A step segments due to the diamond structure of Si(100) [Fig. 4(a)].[17,18] So on the surface quenched from the high temperature ($\gtrsim 950$ K), a lot of S_A step segments contained at the rough S_B step induce strong buckling of dimers, which is expected to form the $p(2\times2)$ phase. While on the surface annealed at low temperature ($\lesssim 950$ K), the

$p(2\times2)$ domains cannot form or the domain size is too small to detect diffraction intensity due to the S_B step fluctuation lower than that of the surface quenched from the high temperature [Fig. 4(b)].

To see the effect of defect density on these reconstructions, we have varied the sputtering conditions we described previously. Only after high-temperature annealing *for two minutes* following Ar^+-ion bombardment, the surface reconstructions mentioned previously reappeared, respectively, depending on their own annealing conditions. Our data show that as long as the annealing temperature is high enough to recover the long-range dimerized surface, the observed reconstructed phases are independent of the ion dose, the ion energy, and the annealing time. This means that the extra defects on two types of terraces generated by sputtering have been almost annihilated. When discussing the annihilation of the extra vacancies, the diffusion anisotropy and the diffusion length of the vacancy should be considered.[19] The activation barrier for the migration of the dimer vacancy along the dimer rows was reported to be 1.5 eV, while the barrier across the dimer rows is 2.2 eV.[19] There is a difference of two orders of magnitude in diffusion rates between two orthogonal directions at the annealing temperature of 1400 K, assuming the preexponential factors are similar. So the dimer vacancy is preferentially moving along the dimer row. Since the dimer vacancies moving along the dimer rows on the A terrace cannot meet the step edges that are believed as a sink of vacancies, the dimer vacancies cannot be annihilated. The annihilation of dimer vacancies on A terraces can be explained with the fluctuation of the S_B step at high temperature to recover the long-range (2×1) reconstruction. At high annealing temperature, the defects on the A terrace are bounded by the long S_A step segments contained at the rough S_B step and the defects moving along dimer rows can be annihilated by the kink. This explanation of defect annihilation by step fluctuation is consistent with the origin of $p(2\times2)$ domains on the surface quenched from high temperature.

In conclusion, we have shown that there are several defect-induced surface reconstructions at the Si(100) surface due to the different annealing conditions. With the high-temperature annealing followed by quenching, we can observe the $p(2\times2)$ and the (2×8) phase. When this surface is annealed at low temperature, the reconstructed two-phase undergoes reversible phase transition to a half-order streak. The sputtering followed by high-temperature annealing for two minutes has no effect on the observed reconstructions. To explain the observed results, the defect distribution and the S_B step fluctuation must be taken into account. For defect distribution, the ordered defect arrangement gives the (2×8) phase while the disordered defect arrangement gives the half-order streak. For the S_B step fluctuation, at high temperature the S_B step fluctuating very highly forms a lot of long S_A step segments which induce the buckling of dimers resulting in a $p(2\times2)$ phase and serve as the sink of dimer vacancies. The reversible phase transition from the (2×2) and (2×8) phases to the half-order streak or *vice versa* can be explained by the order-disorder transition in the defect distribution and the extent of step fluctuation. We have proposed two model surfaces that can explain the observed reconstructions and reversible phase transition.

This work was supported by the Ability Enhancement project at Materials Evaluation Center, Korea Research Institute of Standards and Science. Also, part of this work is supported by the Center for Molecular Science at KAIST. We would like to thank J. H. Kim for his contribution in technical support at KRISS.

*Author to whom all correspondence should be addressed.

[1]E. Artacho and F. Ynduráin, Phys. Rev. Lett. **62**, 2491 (1989).
[2]R. A. Wolkow, Phys. Rev. Lett. **68**, 2636 (1992).
[3]R. J. Hamers, R. M. Tromp, and J. E. Demuth, Phys. Rev. B **34**, 5343 (1986); R. M. Tromp, R. J. Hamers, and J. E. Demuth, Phys. Rev. Lett. **55**, 1303 (1985); J. E. Demuth, U. Koehler, and R. J. Hamers, J. Vac. Sci. Technol. A **8**, 214 (1990).
[4]J. J. Lander and J. Morrison, J. Chem. Phys. **37**, 729 (1962).
[5]T. D. Poppendieck, T. C. Ngoc, and M. B. Webb, Surf. Sci. **75**, 287 (1978).
[6]T. Tabata, T. Aruga, and Y. Murata, Surf. Sci. **179**, L63 (1987).
[7]Y. Enta, S. Suzuki, and S. Kono, Phys. Rev. Lett. **65**, 2704 (1990).
[8]M. J. Cardillo and G. E. Becker, Phys. Rev. B **21**, 1497 (1980).
[9]W. Weiss, D. Schmeisser, and W. Göpel, Phys. Rev. Lett. **60**, 1326 (1988).
[10]J. A. Martin, D. E. Savage, W. Moritz, and M. G. Lagally, Phys. Rev. Lett. **56**, 1936 (1986).
[11]T. Aruga and Y. Murata, Phys. Rev. B **34**, 5654 (1986).
[12]D. J. Chadi, Phys. Rev. Lett. **59**, 1691 (1987).
[13]J. Ihm, D. H. Lee, J. D. Joannopoulos, and J. J. Xiong, Phys. Rev. Lett. **51**, 1872 (1983).
[14]K. Pandey, in *Proceedings of the Seventeenth International Conference on the Physics of Semiconductors,* edited by D. J. Chadi and W. A. Harrison (Springer-Verlag, New York, 1985), p. 55.
[15]H. S. Kim, K. C. Low, and C. K. Ong, Phys. Rev. B **48**, 1595 (1993).
[16]O. L. Alerhand and E. J. Mele, Phys. Rev. B **35**, 5533 (1987).
[17]O. L. Alerhand, A. N. Berker, J. D. Joannopoulos, D. Vanderbilt, R. J. Hamers, and J. E. Demuth, Phys. Rev. Lett. **64**, 2406 (1990); B. S. Swartzentruber, Y.-W. Mo, R. Kariotis, M. G. Lagally, and M. B. Webb, *ibid.* **65**, 1913 (1990).
[18]N. Kitamura, B. S. Swartzentruber, M. G. Lagally, and M. B. Webb, Phys. Rev. B **48**, 5704 (1993); H. J. W. Zanvliet, H. B. Elswijk, and E. J. van Loenen, Surf. Sci. **272**, 264 (1992).
[19]N. Kitamura, M. G. Lagally, and M. B. Webb, Phys. Rev. Lett. **71**, 2082 (1993); Z. Zhang, H. Chen, B. C. Bolding, and M. G. Lagally, *ibid.* **71**, 3677 (1993).

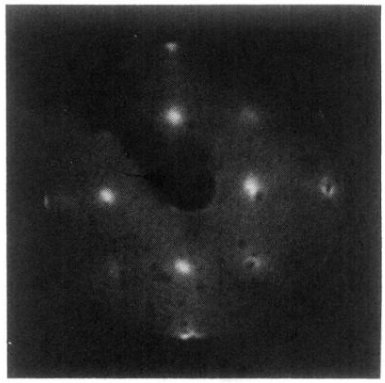

(a)

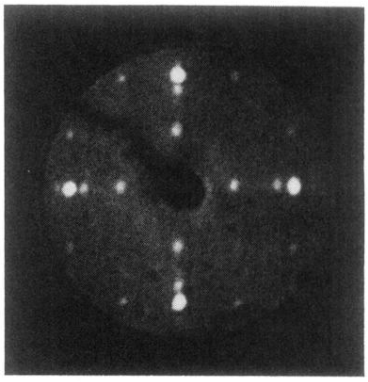

(b)

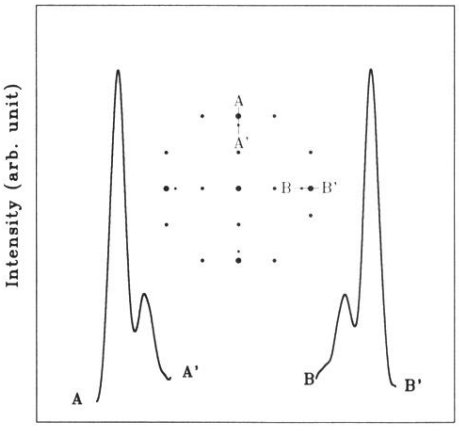

(c)

FIG. 2. The photographs and line profile of a LEED pattern for radiation quenched surface. (a) (2×2) at $E=23$ eV. (b) (2×8) at $E=39$ eV. (c) The line profile of a (2×8) LEED pattern represented in (b). The line scan direction is shown in the inset of (c), where the inset is schematic of photograph of (b).

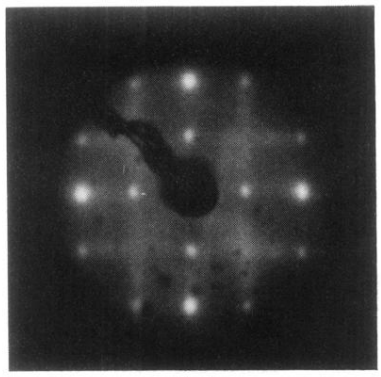

(a)

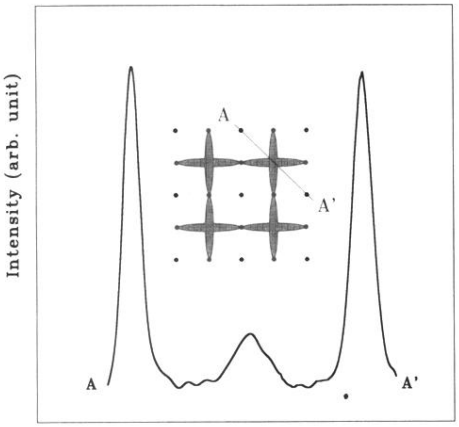

(b)

FIG. 3. The photograph and line profile for a slow-cooled surface. (a) The LEED pattern of half-order streaks at $E=39$ eV. (b) The line profile of this LEED pattern from the direction represented in the inset of (b).